A Multi-Head Self-Attention Mechanism for Improved Brain Tumor Classification using Deep Learning Approaches

Prasadu Reddi
Computer Science and Systems Engineering, AU-TDR-HUB, Andhra University, Visakhapatnam, India | Department of Information Technology,ANITS(A), Visakhapatnam,Visakhapatnam,India
reddiprasad0112@gmail.com (corresponding author)

Gorla Srinivas
Computer Science & Engineering, GITAM Deemed to be University, Visakhapatnam, India
sgorla@gitam.edu

P. V. G. D. Prasad Reddy
Computer Science & Systems Engineering, Andhra University, Visakhapatnam, India
prasadreddyvizag@gmail.com

Dasari Siva Krihsna
Computer Science & Engineering, GITAM Deemed to be University, Visakhapatnam, India
sivadasari120891@gmail.com

Received: 24 July 2024 | Revised: 17 August 2024 | Accepted: 29 August 2024

Licensed under a CC-BY 4.0 license | Copyright (c) by the authors | *DOI: https://doi.org/10.48084/etasr.8484*

ABSTRACT

One of the most common life-threatening diseases, the brain tumor is a condition characterized by the rapid proliferation of abnormal cells that leads to the destruction of healthy brain cells. Its aggressive nature can result in a patient succumbing to the disease before an accurate diagnosis is achieved. Timely detection is crucial to effective treatment and patient survival. Similarly, early detection plays a pivotal role in the case of brain tumors, where swift identification is vital to providing optimal care and increasing the chances of patient recovery. Streamlining the complex process of brain tumor detection is a significant undertaking that aims to simplify and expedite the procedure, ultimately contributing to saving valuable time and enhancing patient outcomes. The proposed model, a modified VGG-16, facilitates faster and more accurate identification of abnormal brain cells, leading to early detection of brain tumors. A novel multihead self-attention mechanism is used in the modified VGG-16 architecture to improve tumor detection performance. The proposed model performs better than other state-of-the-art models, such as normal VGG-16, ResNet-50, and EfficientNet.

Keywords-VGG-16; ResNet-50; EfficientNet; modified VGG-16; multi-head self attention mechanism

I. INTRODUCTION

Brain tumors represent a devastating and often fatal form of cancer that affects individuals across various age groups, including both children and adults. This malignancy arises from abnormal proliferation of cells within the brain, posing a considerable threat to life. Medical professionals commonly rely on Magnetic Resonance Imaging (MRI) to examine and identify brain tumors. However, the intricate and interconnected structure of the brain presents challenges in achieving accurate diagnoses. Efficient and early diagnosis, as well as the classification of brain tumors into specific categories, is of paramount importance [1-3]. Brain tumors fall into two primary categories: primary and secondary. Primary tumors originate within the brain, while secondary tumors result from cells that originate elsewhere in the body [4]. Primary brain tumors are classified into benign and malignant. Benign tumors exhibit slower growth rates and less aggressive infiltration into surrounding tissues compared to malignant brain tumors. Malignant tumors, on the other hand, can be easily identified due to distinct intensity differences from adjacent cells [5-7].

Quantitatively predicting tumor progression using patient data plays a crucial role in clinical decision-making, particularly during therapy planning and tumor staging. Brain tumors present segmentation challenges due to their variable shape, exterior, and position [8-9]. Segmentation methods can be classified as automatic or semi-automatic, with the latter requiring user interaction [10]. Given the inherent noise in MRI data, constant filtering is necessary to remove high-frequency disturbances before processing [11-13]. Automatic segmentation traditionally employs conventional machine learning models, often incorporating handcrafted features. In recent times, Convolutional Neural Networks (CNNs) have gained prominence in brain tumor segmentation, enabling the extraction of more sophisticated features from brain images. This study aims to advance tumor growth segmentation through optimized modeling and the application of Deep Learning (DL) algorithms. A modified VGG-16 is used to enhance the accuracy and efficiency of the segmentation process, contributing to improved results in the field of brain tumor prognosis and diagnosis. The contributions of this work include the following:

- The modified VGG-16 model with the integrated multi-head self-attention mechanism advances the field of brain tumor classification.
- The proposed method shows superior performance compared to other state-of-the-art models, including VGG-16, ResNet-50, and EfficientNet.
- Experimental analysis to evaluate the proposed approach using four distinct metrics reveals promising results in terms of accuracy, precision, recall, and F1 score values.

II. RELATED WORKS

Previous studies in brain tumor classification predominantly employed traditional machine-learning algorithms. In [15], feature engineering and handcrafted features were used to distinguish between different tumor types. However, these approaches often struggle to capture complex patterns inherent in medical imaging data. DL methods, particularly CNNs, have shown remarkable success in medical image analysis, as previous studies demonstrated the effectiveness of CNNs in automatically learning hierarchical features for brain tumor classification. Despite their success, these studies did not explore the potential of LLMs, as recent advances integrated LLMs into various medical imaging tasks. In [5], LLMs were used for feature extraction in radiological images, showing promising results in disease detection. However, to our knowledge, the application of LLMs in brain tumor classification remains an underexplored area.

In [16, 17], majority voting and deep hybrid models were proposed for improved prediction. In [18, 19] feature selection approaches with embedding techniques were examined. In [20, 21], cloud-based architectures were used to improve sound classification using artificial neural networks. In [22], a cat swarm optimization-based approach was proposed with a U-Net-based segmentation mechanism for skin cancer detection. In [23], mental conditions were explored using machine and DL approaches. Transfer learning has been a pivotal concept in medical imaging. In [7], the efficacy of pre-trained models was demonstrated on large datasets for general medical image classification. In [24], an early breast cancer diagnosis system was proposed using a CNN architecture. In [25], lung cancer detection was based on DL approaches such as CNN, VGG-16, and VGG-19. In [26], multichannel hybrid deep neural networks were proposed for avocado ripeness classification, using VGG-16 and EffiecientNetB0.

III. PROPOSED METHOD

The proposed method consists of various stages that include preprocessing, modified VGG-16 with multi-head self-attention, and a fully connected layer with a softmax function for tumor detection. Figure 1 shows the workflow of the proposed architecture.

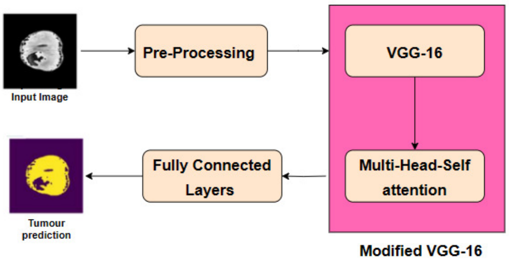

Fig. 1. Workflow of the method.

A. VGG-16 Architecture

VGG16 is a deep CNN architecture that has proven effective in various computer vision tasks, including image classification. The VGG16 architecture consists of several convolutional layers followed by fully connected layers. VGG16 has five convolutional blocks, each containing multiple convolutional layers followed by max-pooling layers.

- Convolutional Layers: The convolutional layers in VGG-16 are denoted as $Conv(n, (k,k), \ activation = relu)$, where n is the number of filters, (k,k) is the filter size, and $activation = relu$ indicates the Rectified Linear Unit (ReLU) activation function. For a given convolutional layer l, let $\mathrm{X}[l]$ be the input, $W[l]$ be the filter weights, $\mathrm{b}[l]$ be the bias term, and $\mathrm{A}[l]$ be the output after activation. The mathematical representation of a convolutional layer is given by:

$$\mathrm{Z}[l] = \mathrm{W}[l] * \mathrm{X}[l] + \mathrm{b}[l] \quad (1)$$

where, $*$ denotes the convolution operation, and $ReLU(x) = max(0, x)$ is the ReLU function.

- MaxPooling Layer: The max-pooling operation downsamples the spatial dimensions of the input tensor. For a given max-pooling layer l, the operation is defined as:

$$MaxPooling\big((f,f)\big)\mathrm{A}[\mathrm{l}] \quad (2)$$

This operation extracts the maximum value from each $f \times f$ region in the input.

- Fully Connected Layers: The fully connected layers are denoted as $Dense(n, \ activation = relu)$ or $Dense(1, \ activation = sigmoid)$, where n is the number of neurons and the activation function is either the ReLU or the sigmoid function. For a given fully connected layer l, let $\mathrm{A}[l]$ be the input, $\mathrm{W}[l]$ be the weight matrix, $\mathrm{b}[l]$ be the bias term, and $\mathrm{A}[l+1]$ be the output after activation. The mathematical representation of a fully connected layer is given by:

$$\mathrm{Z}[l+1] = \mathrm{W}[l+1].\mathrm{A}[l] + \mathrm{b}[l+1] \quad (3)$$

$$\mathrm{A}[l+1] = ReLU(\mathrm{Z}[l+1]) \quad (4)$$

where · denotes the matrix multiplication, and $\sigma(x)$ is the sigmoid activation function.

B. ResNet-50 Architecture

ResNet-50 for brain tumor classification involves adapting the architecture to suit binary classification.

- Residual Block: The fundamental building block in ResNet is the residual block, defined as follows. Given an input $\mathrm{X}[l]$, the residual block consists of:

  Shortcut Connection:

  $$Shortcut(\mathrm{X}[l]) = \mathrm{X}[l] \quad (5)$$

  Main Path:

  $$\mathrm{Z1}[l] = Conv(\mathrm{X}[l], \mathrm{W1}[l]) \quad (6)$$

  $$\mathrm{A1}[l] = BatchNorm(\mathrm{Z1}[l]) \quad (7)$$

  $$\mathrm{A1}[l] = ReLU(\mathrm{A1}[l]) \quad (8)$$

  $$\mathrm{Z2}[l] = Conv(\mathrm{A1}[l], \mathrm{W2}[l]) \quad (9)$$

  $$\mathrm{A2}[l] = BatchNorm(\mathrm{Z2}[l]) \quad (10)$$

  $$\mathrm{A2}[l] = \mathrm{A2}[l] + Shortcut(\mathrm{X}[l]) \quad (11)$$

  $$A[l+1] = ReLU(A2[l]) \quad (12)$$

Here, $Conv(X, W)$ represents the convolutional operation with weights W, and $BatchNorm(\mathrm{X})$ is the batch normalization operation.

C. EfficientNet Architecture

This architecture describes a family of CNNs that are designed to achieve high accuracy while being computationally efficient. EfficientNet addresses the challenge of scaling neural networks to achieve better performance without significantly increasing computational complexity. The key idea behind EfficientNet is to balance the depth, width, and resolution of the model to optimize overall efficiency. EfficientNet can be advantageous for the classification of brain tumors or any medical image analysis task because of its ability to provide strong performance with fewer parameters. The compound scaling formula is expressed by

$$d = \alpha^{\phi}, w = \beta^{\phi}, r = \gamma^{\phi} \quad (13)$$

where α, β, and γ are constants, and ϕ is a user-defined parameter that controls the trade-off between model size and accuracy.

IV. PROPOSED MODEL

The proposed method consists of various stages that include preprocessing, modified VGG-16 with multi-head self-attention, and a fully connected layer with softmax function for tumor detection.

A. Preprocessing

Preprocessing plays a crucial role in preparing medical images, such as brain tumor images, for analysis and diagnosis. This study used image rescaling and normalization to ensure that the images are on a consistent scale and have comparable intensity levels, which is often important in tumor classification. Pixel values are scaled based on the range of values in the original image, mapping them to a normalized range.

- Image Rescaling: This process involves adjusting the size or resolution of an image and is often performed to standardize the dimensions of images in a dataset. This process typically involves interpolation to estimate pixel values at the new resolution. The mathematical equation for rescaling an image can be expressed as

  $$I_{rescaled}(x, y) = I\left(\frac{x}{s_x}, \frac{y}{s_y}\right) \quad (14)$$

  where $I_{rescaled}(x, y)$ is the pixel value at coordinates (x, y) in the rescaled image, $I(x, y)$ is the original pixel value at coordinates $(x/s_x, y/s_y)$, and s_x and s_y are scaling factors for the x and y dimensions, respectively.

- Image normalization: This involves scaling pixel values to a standardized range, often between 0 and 1 or -1 and 1. This is done to ensure that pixel values have a consistent scale, which can be important for training machine learning models. The normalization equation is given by

  $$I_{normalized}(x, y) = \frac{I(x,y) - \min(I)}{\max(I) - \min(I)} \quad (15)$$

B. VGG-16 with Multihead Attention

Combining VGG16 with multi-head attention is an interesting approach to enhance the model's ability to capture complex relationships within brain tumor images. Multihead attention is commonly associated with transformer architectures, but it can be adapted to enhance the feature extraction capabilities of CNNs such as VGG16. The proposed architecture showcases the extracted features from each block. The extracted features are fed to the multi-head self-attention mechanism, in which the model concatenates the features and supplies them to the fully connected layer. Then, the flattened features are fed to the softmax for the prediction. Figure 2 shows the modified VGG16 architecture.

- Attention Mechanism: The attention mechanism can be represented using the following equations for a single attention head: Given an input $\mathrm{X}[l]$ (output of the previous layer), the attention mechanism computes the attention matrix $\mathrm{A}[l]$ as follows:

  Query, Key, and Value Projections by:

  $$\mathrm{Q}[l] = \mathrm{X}[l]\,.\,\mathrm{W}_q[\mathrm{l}] \quad (16)$$

$$K[l] = \mathrm{X}[l]\,.\,\mathrm{W}_k[l] \tag{17}$$

$$\mathrm{V}[l] = \mathrm{X}[l]\,.\ \mathrm{W}_v[l] \tag{18}$$

where $\mathrm{W}_q[l]$, $\mathrm{W}_k[l]$, and $\mathrm{W}_v[l]$ are learnable weight matrices. The scaled dot-product attention is given by

$$Attention(\mathrm{Q}[l], \mathrm{K}[l], \mathrm{V}[l]) = Softmax\left(\frac{\mathrm{Q}[l].(\mathrm{K}[l])^{\mathrm{T}}}{\sqrt{d_k}}\right).\mathrm{V}[l] \tag{19}$$

where d_k is the dimensionality of the key vectors.

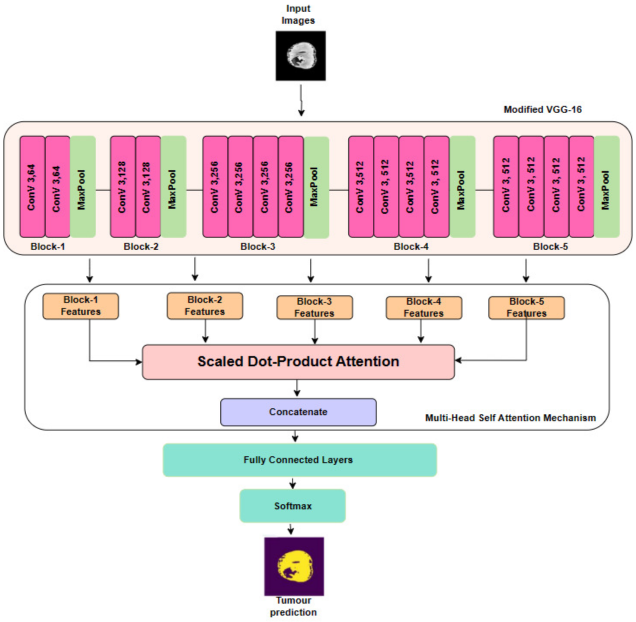

Fig. 2. Modified VGG-16 architecture.

- Multihead Attention: The outputs from multiple attention heads are concatenated and linearly transformed as

$$MultiHead(\mathrm{X}[l]) = Concat(head_1, \dots, head_{\mathrm{h}}) \cdot \mathrm{WO} \tag{20}$$

where WO is another learnable weight matrix.

- Modified Fully Connected Layers: After the attention mechanism, the output is passed through the fully connected layers as

$$\mathrm{Z}[l+1] = Multihead(\mathrm{X}[l]) \cdot \mathrm{W}[l+1] + \mathrm{b}[l+1] \tag{21}$$

$$\mathrm{A}[l+1] = ReLU(\mathrm{Z}[l+1]) \tag{22}$$

where $\mathrm{W}[l+1]$ is the weight matrix and $\mathrm{b}[l+1]$ is the bias term.

The entire model involves stacking convolutional layers (VGG16) followed by a flattened layer. Then, the attention mechanism is applied, and the output is processed through fully connected layers.

V. EXPERIMENTAL ANALYSIS

The proposed modified VGG-16 with a multihead self-attention mechanism was compared with other models, such as VGG-16, ResNet50, and EfficientNet.

A. Dataset Description

This study used the BRATS 2018, BRATS 2019, and BRATS 2020 datasets for tumor detection. BRATS 2018 consists of 240 HGG features and 70 LGG features, BRATS 2019 consists of 280 HGG features and 80 LGG features, and BRATS 2020 consists of 151 HGG features and 70 LGG features. All three datasets were combined into a single dataset for performance analysis. The combined BRATS 2018, 2019, and 2020 dataset consists of 671 HGG features and 220 LGG features. The datasets were divided into 80:20 for training and testing, respectively.

B. Hyperparameters

- VGG-16: Input images of size 224×224 pixels, 13 convolutional layers, all with 3x3 filter size, five max-pooling layers with 2x2 pool size and stride 2, and three fully connected layers, The first two fully connected layers have 4096 neurons each, ReLU activation function. Dropout is applied with a probability of 0.5 and softmax activation.

- ResNet-50: Input images of size 224×224 pixels, 50 convolutional layers, all with 3x3 filter size. ResNet-50 uses bottleneck blocks with three convolutional layers (1×1, 3x3, 1x1) to reduce computational complexity. Each bottleneck block has a shortcut connection (skip connection) that skips one or more layers, max-pooling with a 3x3 pool size and stride 2 is used at the beginning, and global average pooling is used before the final output layer and ReLU activation function. Stochastic Gradient Descent (SGD) such as Adam is used as an optimizer.

- EfficientNet: Input images of size 224×224 pixels. EfficientNet introduces compound scaling to balance the model depth, width, and resolution. The model is scaled by a factor (phi) to achieve different model sizes. B0: depth = 1.0, width = 1.0, resolution = 224×224, and seven convolutional blocks. Dropout is applied with a probability of 0.5. Batch normalization and ReLU activation are used. The learning rate is 0.08. SGD Adam is used as an optimizer.

C. Evaluation Metrics

Accuracy (Acc), Precision (Pre), Recall (RC - Sensitivity), and F1-score (F1) are commonly used to assess the effectiveness of classification models. Accuracy (Acc) measures the overall correctness of the model predictions

$$Accuracy = \frac{TP+TN}{TP+TN+FP+FN}$$

Precision (Pre) measures the accuracy of the positive predictions

$$Precision = \frac{TP}{TP+FP}$$

Recall (RC) measures the ability of the model to capture all positive instances

$$Recall = \frac{TP}{TP+FN}$$

F1 score (F1) is the harmonic mean of precision and recall, providing a balanced measure between them.

$$F1 - Score = \frac{2.Precision.Recall}{Precision+Recall}$$

D. Performance Analysis

The proposed method exhibited superior performance in both the individual and the combined dataset, showcasing its effectiveness. It appears to be a robust choice for the given task, offering high accuracy and precision while maintaining a strong balance between recall and F1 score. Tables I-IV show the detailed results of transfer learning approaches and the proposed modified VGG-16 classifier using various datasets. These results demonstrate the effectiveness of the proposed modified VGG16 model, as it achieved significantly improved performance metrics.

TABLE I. PERFORMANCE ANALYSIS ON BRATS 2018

Algorithm	**BRATS 2018 Dataset**			
	Acc	**Pre**	**RC**	**F1**
VGG-16	88.14	80.00	89.29	88.89
ResNet-50	95.55	93.86	93.86	93.86
EfficientNet	97.20	97.68	96.56	97.70
Proposed method	98.06	98.45	97.68	97.70

The proposed method achieves very high accuracy and F1 score, indicating good overall performance. Its precision and recall are also balanced. EfficientNet shows competitive results with high precision. However, the F1 score is slightly lower than VGG-16, suggesting a potential trade-off between precision and recall.

TABLE II. PERFORMANCE ANALYSIS ON BRATS 2019

Algorithm	**BRATS 2019 dataset**			
	Acc	**Pre**	**RC**	**F1**
VGG-16	86.44	77.78	71.43	87.50
ResNet-50	76.27	66.67	66.67	80.00
EfficientNet	86.14	78.00	87.29	86.89
Proposed method	95.55	93.86	83.86	93.86

In this case, the proposed method performs well in terms of accuracy and F1 score. It also shows good precision, but the recall is relatively lower, indicating potential room for improvement in capturing true positives. ResNet-50 has a lower accuracy and F1 score compared to VGG-16 and EfficientNet.

TABLE III. PERFORMANCE ANALYSIS ON BRATS 2020

Algorithm	**BRATS 2020 dataset**			
	Acc	**Pre**	**RC**	**F1**
VGG-16	92.20	90.48	90.48	90.48
ResNet-50	88.14	88.89	85.71	87.27
EfficientNet	91.53	89.66	92.86	91.23
Proposed method	97.20	97.68	96.56	97.70

The proposed modified VGG-16 model performs well with high accuracy, precision, recall, and F1 score on the BRATS 2020 dataset, showing balanced performance in capturing TP and avoiding FP.

The proposed modified VGG-16 maintains a high level of performance in the combined dataset, with balanced accuracy, precision, recall, and F1 score, demonstrating consistent effectiveness across different datasets. ResNet-50 also shows robust performance in the combined dataset with high accuracy and precision, although it has slightly lower recall and F1 scores compared to the original VGG-16.

TABLE IV. PERFORMANCE ANALYSIS ON COMBINED BRATS 2018, 2019, AND 2020 DATASET

Algorithm	**Combined dataset: BRATS 2018,2019, and 2020**			
	Acc	**Pre**	**RC**	**F1**
VGG-16	94.55	92.86	92.86	92.86
ResNet-50	94.06	93.83	90.48	92.12
EfficientNet	92.20	90.48	90.48	90.48
Proposed method	98.06	98.45	97.68	97.70

VI. CONCLUSION

Brain tumors are a life-threatening condition that requires timely detection and swift diagnosis to achieve optimal patient outcomes. The proposed model, a modified VGG-16 architecture with a novel multi-head self-attention mechanism, aims to streamline and expedite the complex process of brain tumor detection. Early detection is essential in enhancing treatment effectiveness and patient recovery rates. This study underscores the significance of the integrated multi-head self-attention mechanism in the VGG-16 model, showcasing its ability to improve classification accuracy. This approach outperforms established models such as VGG-16, ResNet-50, and EfficientNet, marking a substantial advancement in brain tumor detection methods. By achieving superior performance metrics, the proposed modified VGG-16 model with multi-head self-attention emerges as a promising innovation in healthcare. This research not only contributes to the technical landscape of medical diagnostics but also has tangible implications for patient care and improved outcomes. Ultimately, this study represents a significant step toward more efficient and accurate brain tumor detection, presenting a potential breakthrough in ongoing efforts to advance diagnostic capabilities in the realm of life-threatening diseases.

REFERENCES

[1] M. Sajjad, S. Khan, K. Muhammad, W. Wu, A. Ullah, and S. W. Baik, "Multi-grade brain tumor classification using deep CNN with extensive data augmentation," *Journal of Computational Science*, vol. 30, pp. 174–182, Jan. 2019, https://doi.org/10.1016/j.jocs.2018.12.003.

[2] Z. U. Rehman, M. S. Zia, G. R. Bojja, M. Yaqub, F. Jinchao, and K. Arshid, "Texture based localization of a brain tumor from MR-images by using a machine learning approach," *Medical Hypotheses*, vol. 141, Aug. 2020, Art. no. 109705, https://doi.org/10.1016/j.mehy.2020.109705.

[3] F. Özyurt, E. Sert, E. Avci, and E. Dogantekin, "Brain tumor detection based on Convolutional Neural Network with neutrosophic expert maximum fuzzy sure entropy," *Measurement*, vol. 147, Dec. 2019, Art. no. 106830, https://doi.org/10.1016/j.measurement.2019.07.058.

[4] C. Mantia and J. I. Zwicker, "Anticoagulation in the Setting of Primary and Metastatic Brain Tumors," in *Thrombosis and Hemostasis in Cancer*, G. Soff, Ed. Cham, Switzerland: Springer International Publishing, 2019, pp. 179–189.

[5] S. S. Veer Handore, A. Deshpande, and P. M. Patil, "An Efficient Algorithm for Segmentation and Classification of Brain Tumor," in *2018 International Conference On Advances in Communication and Computing Technology (ICACCT)*, Sangamner, India, Feb. 2018, pp. 83–88, https://doi.org/10.1109/ICACCT.2018.8529611.

[6] N. Singh and S. Goyal, "Determination and Segmentation of Brain Tumor Using Threshold Segmentation with Morphological Operations," in *Soft Computing: Theories and Applications*, Singapore, 2018, pp. 715–726, https://doi.org/10.1007/978-981-10-5699-4_68.

[7] M. Mudda, R. Manjunath, and N. Krishnamurthy, "Brain Tumor Classification Using Enhanced Statistical Texture Features," *IETE Journal of Research*, vol. 68, no. 5, pp. 3695–3706, Sep. 2022, https://doi.org/10.1080/03772063.2020.1775501.

[8] K. Usman and K. Rajpoot, "Brain tumor classification from multi-modality MRI using wavelets and machine learning," *Pattern Analysis and Applications*, vol. 20, no. 3, pp. 871–881, Aug. 2017, https://doi.org/10.1007/s10044-017-0597-8.

[9] J. Amin, M. Sharif, N. Gul, M. Yasmin, and S. A. Shad, "Brain tumor classification based on DWT fusion of MRI sequences using convolutional neural network," *Pattern Recognition Letters*, vol. 129, pp. 115–122, Jan. 2020, https://doi.org/10.1016/j.patrec.2019.11.016.

[10] A. R. Raju, P. Suresh, and R. R. Rao, "Bayesian HCS-based multi-SVNN: A classification approach for brain tumor segmentation and classification using Bayesian fuzzy clustering," *Biocybernetics and Biomedical Engineering*, vol. 38, no. 3, pp. 646–660, Jan. 2018, https://doi.org/10.1016/j.bbe.2018.05.001.

[11] S. Banerjee and G. K. Singh, "Quality Aware Compression of Multilead Electrocardiogram Signal using 2-mode Tucker Decomposition and Steganography," *Biomedical Signal Processing and Control*, vol. 64, Feb. 2021, Art. no. 102230, https://doi.org/10.1016/j.bspc.2020.102230.

[12] S. Banerjee and G. K. Singh, "A new approach of ECG steganography and prediction using deep learning," *Biomedical Signal Processing and Control*, vol. 64, Feb. 2021, Art. no. 102151, https://doi.org/10.1016/j.bspc.2020.102151.

[13] S. Banerjee and G. K. Singh, "Deep neural network based missing data prediction of electrocardiogram signal using multiagent reinforcement learning," *Biomedical Signal Processing and Control*, vol. 67, May 2021, Art. no. 102508, https://doi.org/10.1016/j.bspc.2021.102508.

[14] M. Havaei *et al.*, "Brain tumor segmentation with Deep Neural Networks," *Medical Image Analysis*, vol. 35, pp. 18–31, Jan. 2017, https://doi.org/10.1016/j.media.2016.05.004.

[15] K. Popuri, D. Cobzas, A. Murtha, and M. Jägersand, "3D variational brain tumor segmentation using Dirichlet priors on a clustered feature set," *International Journal of Computer Assisted Radiology and Surgery*, vol. 7, no. 4, pp. 493–506, Jul. 2012, https://doi.org/10.1007/s11548-011-0649-2.

[16] D. S. Krishna, G. Srinivas, and P. V. G. D. Prasad Reddy, "Disaster tweet classification: A majority voting approach using machine learning algorithms," *Intelligent Decision Technologies*, vol. 17, no. 2, pp. 343–355, Jan. 2023, https://doi.org/10.3233/IDT-220310.

[17] D. S. Krishna, G. Srinivas, and P. V. G. D. Prasad Reddy, "A Deep Parallel Hybrid Fusion Model for disaster tweet classification on Twitter data," *Decision Analytics Journal*, vol. 11, Jun. 2024, Art. no. 100453, https://doi.org/10.1016/j.dajour.2024.100453.

[18] S. K. Dasari, G. Srinivas, and P. V. G. D. Prasad Reddy, "A Comprehensive Study on Disaster Tweet Classification on Social Media Information," in *Soft Computing and Signal Processing*, Singapore, 2024, pp. 507–516, https://doi.org/10.1007/978-981-99-8628-6_43.

[19] S. K. Dasari, L. Sravani, M. U. Kumar, and N. Rama Venkata Sai, "Image Enhancement of Underwater Images Using Deep Learning Techniques," in *Proceedings of International Conference on Data Analytics and Insights, ICDAI 2023*, Kolkata, India, May 2023, pp. 715–730, https://doi.org/10.1007/978-981-99-3878-0_61.

[20] S. K. Dasari, S. K. Kella, and R. Manda, "Enhancing Environmental Sounds Classification through Deep Learning Techniques," in *2023 International Conference on Sustainable Computing and Data Communication Systems (ICSCDS)*, Erode, India, Mar. 2023, pp. 265–270, https://doi.org/10.1109/ICSCDS56580.2023.10104722.

[21] D. S. Krishna, G. Srinivas, and P. V. G. D. P. Reddy, "Novel private cloud architecture: A three tier approach to deploy private cloud using virtual machine manager," *Intelligent Decision Technologies*, vol. 17, no. 2, pp. 275–285, Jan. 2023, https://doi.org/10.3233/IDT-229035.

[22] V. A. Rajendran and S. Shanmugam, "Automated Skin Cancer Detection and Classification using Cat Swarm Optimization with a Deep Learning Model," *Engineering, Technology & Applied Science Research*, vol. 14, no. 1, pp. 12734–12739, Feb. 2024, https://doi.org/10.48084/etasr.6681.

[23] B. H. Bhavani and N. C. Naveen, "An Approach to Determine and Categorize Mental Health Condition using Machine Learning and Deep Learning Models," *Engineering, Technology & Applied Science Research*, vol. 14, no. 2, pp. 13780–13786, Apr. 2024, https://doi.org/10.48084/etasr.7162.

[24] A. Naz, H. Khan, I. U. Din, A. Ali, and M. Husain, "An Efficient Optimization System for Early Breast Cancer Diagnosis based on Internet of Medical Things and Deep Learning," *Engineering, Technology & Applied Science Research*, vol. 14, no. 4, pp. 15957–15962, Aug. 2024, https://doi.org/10.48084/etasr.8080.

[25] S. T. Vemula, M. Sreevani, P. Rajarajeswari, K. Bhargavi, J. M. R. S. Tavares, and S. Alankritha, "Deep Learning Techniques for Lung Cancer Recognition," *Engineering, Technology & Applied Science Research*, vol. 14, no. 4, pp. 14916–14922, Aug. 2024, https://doi.org/10.48084/etasr.7510.

[26] S. Nuanmeesri, "Utilization of Multi-Channel Hybrid Deep Neural Networks for Avocado Ripeness Classification," *Engineering, Technology & Applied Science Research*, vol. 14, no. 4, pp. 14862–14867, Aug. 2024, https://doi.org/10.48084/etasr.7651.